Kinematic Analysis of Translational 3-DOF Micro Parallel Mechanism Using Matrix Method

Yoshihiko KOSEKI, Tamio TANIKAWA, and Noriho KOYACHI
Mechanical Engineering Laboratory,
AIST, MITI
1-2 Namiki, Tsukuba, Ibaraki 305-8564,
Japan
{koseki, tamio, koyachi}@mel.go.jp

Tatsuo ARAI
Graduate School of Engineering Science,
Osaka University
1-3 Machikaneyama-machi, Toyonaka,
Osaka 560-8531, Japan
arai@sys.es.osaka-u.ac.jp

Abstract

In this paper, we applied the matrix method to kinematic analysis of our translational 3-DOF (Degrees Of Freedom) micro parallel mechanism for an instance of general flexure mechanisms. The matrix method has been well developed in architecture to analyze a frame structure. We found that this method is well applicable to such a flexure mechanism with circular notched hinges as our micro parallel mechanism because it is approximate to a Rahmen structure. Our matrix method can calculate a compliance matrix with less nodes of matrix than conventional FEM (Finite Element Method). Firstly, the compliance matrices of a circular notched hinge and some other beams are defined and the coordinate transformations of compliance matrix are introduced. Secondly, an analysis of our micro parallel mechanism is demonstrated.

1 Introduction

A flexure mechanism that has some notched hinges has been widely used for micro-precision machinery, like a micropositioning stage, accelerometer, and micromanipulator. The notched hinge is made a circular or rectangular notch and is totally thick but partially thin beam (See Fig. 2(c)). So it is compliant in bending around one axis along notch but rigid around the other axes. So it works approximately as an angular axis. The merits of this hinge are vacuum compatibility, no backlash property, no non-linear friction, simple structure and easy manufacture. However, insufficient flexibility around rotation axis and/or insufficient stiffness around other axes cause non-intended motion of the output. An analysis of the hinge and total mechanism is necessary for accurate motion and optimal design.

The analysis of flexure hinge mechanism has a long history. The analytic formulations of circular notched hinge were firstly given by Paros [1]. Yoshimura corrected the mistake in Paros' approximation $\triangle x/F_x$ and analyzed other types of hinge [2]. Rong analyzed and tested the error effect of their micro-motion stage [3]. Her also analyzed closed-loop micro-positioning stage while treating each hinge as torsion spring [4]. Hara proposed micro-parallel mechanism with flexure pivot and hinge [5]. Hara's mechanism is different from the others in the respect that it is not a plane but a spatial mechanism.

In previous works, the full set of deformation of hinge was analyzed but they were neglected or only deformation around one axis was considered in the analysis of total mechanism. Furthermore, the other members than hinge are assumed as rigid and their deformations were neglected.

The matrix method has been well developed in architecture to analyze such a frame structure as bridges (E.g. [6, 7]). This method is applicable to the flexure mechanisms because they can be treated as a Rahmen structure. The matrix method is advantageous because it can deal with full set of deformation of all mechanical members. In addition, different from FEM (FEM is also a kind of matrix method), our method needs much less nodes of matrix. That means less computer power and rapid calculation. In this method, the linear relationship between force and deformation is established (Hook's law). The translational and rotational displacements are also linearized because they are small.

As mentioned above, this method has already been well developed, so we would just demonstrate this method by applying to our translational 3-DOF micro parallel mechanism [8], which need spatial error analysis of hinges and other members.

2 Compliance & Stiffness Matrix Method

Here, it is assumed that the linear relation is established between force and deformation. When forces and moments in/around certain axes are exerted on a certain point, the infinitesimal translational and rotational displacements of that point are formulated as Eq. (1) and Eq. (2). Note that the set of forces and

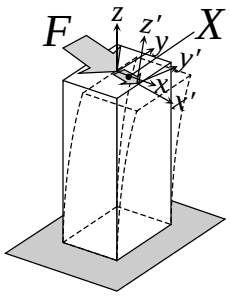

Figure 1: Compliance/Stiffness Matrix

moments, the set of translational and rotational displacements are expressed as F and X, respectively. Hereafter, the force and moment, translational and rotational displacement will not be distinguished.

$$X = \overline{C}\,F \tag{1}$$

$$F = \overline{K}\,X \tag{2}$$

The matrix $\overline{C}$ is called as compliance matrix or flexibility matrix, and the matrix $\overline{K}$ is called as stiffness matrix. $\overline{C}$ and $\overline{K}$ are inverse matrices of each other, and both are regular and symmetric.

2.1 Compliance Matrix of Beams

Eq. (3) shows the displacement of the tip of general beam when external forces are exerted on it. f_n and δ_n are the force and translational displacement in n-axis, respectively and M_n and θ_n are the moment and rotational displacement around n-axis, respectively. The c_i $(i = 1 \dots 8)$ are shown in Table 1 in case of a cylinder, prismatic beam, right circular notched hinge. They are frequently used in flexure mechanisms. The E and G are modulus of longitudinal elasticity (Young's modulus) and modulus of transverse elasticity, respectively and other notations are shown in Fig. 2.

$$\begin{pmatrix} \delta_x \\ \delta_y \\ \delta_z \\ \theta_x \\ \theta_y \\ \theta_z \end{pmatrix} = \begin{pmatrix} c_1 & 0 & 0 & 0 & c_3 & 0 \\ 0 & c_2 & 0 & -c_4 & 0 & 0 \\ 0 & 0 & c_5 & 0 & 0 & 0 \\ 0 & -c_4 & 0 & c_6 & 0 & 0 \\ c_3 & 0 & 0 & 0 & c_7 & 0 \\ 0 & 0 & 0 & 0 & 0 & c_8 \end{pmatrix} \begin{pmatrix} f_x \\ f_y \\ f_z \\ M_x \\ M_y \\ M_z \end{pmatrix} \tag{3}$$

Table 1: Compliance Matrices of beams

	Cylinder	Prismatic Beam	Circular Notched Hinge
c_1	$\dfrac{4l^3}{3\pi E(r_2^4 - r_1^4)}$	$\dfrac{4l^3}{Ea^3b}$	$\dfrac{9\pi r^{\frac{5}{2}}}{2Ebt^{\frac{5}{2}}} + \dfrac{3\pi r^{\frac{3}{2}}}{2Ebt^{\frac{3}{2}}}$
c_2	c_1	$\dfrac{4l^3}{Eab^3}$	$\dfrac{12\pi r^2}{Eb^3}\left\{\left(\dfrac{r}{t}\right)^{\frac{1}{2}} - \dfrac{1}{4}\right\}$
c_3	$\dfrac{2l^2}{\pi E(r_2^4 - r_1^4)}$	$\dfrac{6l^2}{Ea^3b}$	$\dfrac{9\pi r^{\frac{3}{2}}}{2Ebt^{\frac{5}{2}}}$
c_4	c_3	$\dfrac{6l^2}{Eab^3}$	$\dfrac{12r}{Eb^3}\left\{\pi\left(\dfrac{r}{t}\right)^{\frac{1}{2}} - \dfrac{2+\pi}{2}\right\}$
c_5	$\dfrac{l}{\pi E(r_2^2 - r_1^2)}$	$\dfrac{l}{Eab}$	$\dfrac{1}{Eb}\left\{\pi\left(\dfrac{r}{t}\right)^{\frac{1}{2}} - \dfrac{\pi}{2}\right\}$
c_6	$\dfrac{4l}{\pi E(r_2^4 - r_1^4)}$	$\dfrac{12l}{Eab^3}$	$\dfrac{12}{Eb^3}\left\{\pi\left(\dfrac{r}{t}\right)^{\frac{1}{2}} - \dfrac{2+\pi}{2}\right\}$
c_7	c_6	$\dfrac{12l}{Ea^3b}$	$\dfrac{9\pi r^{\frac{1}{2}}}{2Ebt^{\frac{5}{2}}}$
c_8	$\dfrac{2l}{\pi G(r_2^4 - r_1^4)}$	$\dfrac{l}{Gk_2a^3b}$	$\dfrac{9\pi r^{\frac{1}{2}}}{4Gbt^{\frac{5}{2}}}$

As for the twisting (rotational displacement around z-axis) of prismatic beam, $b > a$ is hold and the k_2 is decided by b/a (See Table 2).

As for the right circular notched hinge, almost factors are formulated by Paros [1]. But c_5 is corrected by Yoshimura [2]. In addition, our c_1 is different from Paros'. The approximation error causes a singularity among c_1, c_3, and c_7. To avoid it, the second approximation of $\dfrac{3\pi r^{\frac{3}{2}}}{2Ebt^{\frac{3}{2}}}$ is taken into consideration.

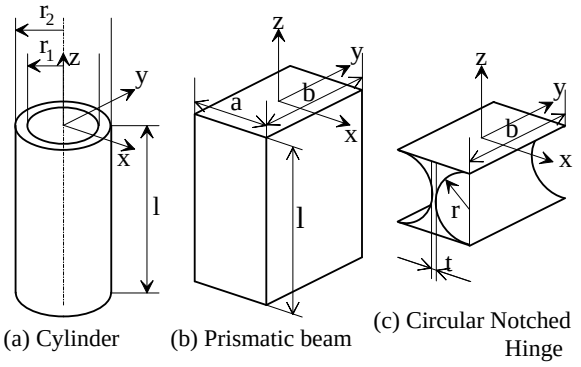

Figure 2: Types of Beam (Cylinder, Prismatic Beam, Circular Notched Hinge)

Table 2: k_2 in Prismatic Beam Twisting

b/a	1.00	2.00	10.00	∞
$k_2(b/a)$	0.141	0.229	0.312	0.333

The twisting factor of circular notched hinge was analyzed by Rong [3]. The specific angle of twist is Eq. (4), while $a = 2r + t - \sqrt{r^2 - z^2}$ and $b > a$.

$$\delta\theta_z = \frac{M_z\,\delta z}{k_2\,G\,a^3\,b} \tag{4}$$

The twisting factor is obtained by integrating Eq. (4).

$$\frac{1}{0.333}\,\frac{M_z\,\delta z}{G\,a^3\,b} \le \delta\theta_z \le \frac{1}{0.141}\,\frac{M_z\,\delta z}{G\,a^3\,b} \tag{5}$$

$$\frac{1}{0.333}\int_{-r}^{r}\frac{M_z\,\delta z}{G\,a^3\,b} < \int_{-r}^{r}\delta\theta_z < \frac{1}{0.141}\int_{-r}^{r}\frac{M_z\,\delta z}{G\,a^3\,b} \tag{6}$$

This calculation is so difficult that the twisting factor is roughly estimated as the following because hinge is usually wide ($b > 2\,r + t$).

$$\theta_z = \frac{9\pi r^{\frac{1}{2}}}{4Gbt^{\frac{5}{2}}}\,M_z \tag{7}$$

2.2 Coordinate Transformation of Compliance Matrix

Firstly, the translational coordinate transformation of compliance matrix is described. When force F is exerted on an object at the point $p = (p_x, p_y, p_z)$ as shown in Fig. 3, the transformed force to the origin F' is obtained as Eq. (8).

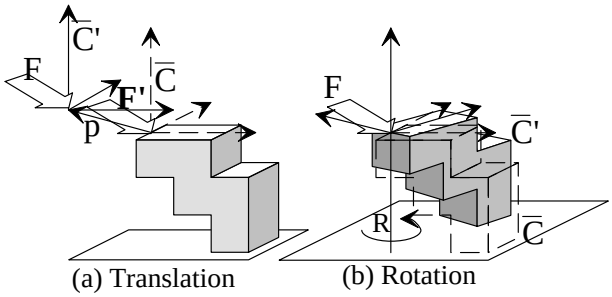

Figure 3: Translation of Compliance Matrix

$$F' = \left(\begin{array}{c|c} I & 0 \\ \hline P & I \end{array}\right) F \tag{8}$$

Note that P expresses the outer product with the vector p. I is an identity matrix.

$$P = \begin{pmatrix} 0 & -p_z & p_y \\ p_z & 0 & -p_x \\ -p_y & p_x & 0 \end{pmatrix} \quad I = \begin{pmatrix} 1 & 0 & 0 \\ 0 & 1 & 0 \\ 0 & 0 & 1 \end{pmatrix}$$

When the object is deformed and its origin moves δX, the point $p = (p_x, p_y, p_z)$, which belongs to the coordinate of the object moves δp. The displacement is linearized because it is infinitesimal.

$$\delta p = \left(\begin{array}{c|c} I & P^T \\ \hline 0 & I \end{array}\right) \delta X \tag{9}$$

Eq. (8), (9) lead new compliance matrix when the origin of the object move to p.

$$\overline{C}' = \left(\begin{array}{c|c} I & P^T \\ \hline 0 & I \end{array}\right) \overline{C} \left(\begin{array}{c|c} I & 0 \\ \hline P & I \end{array}\right) \tag{10}$$

In the same manner, the rotational coordinate transformation shown in Fig. 3(b) is obtained in Eq. (10). The R is a rotational matrix. The force is rotated by $R^T (= R^{-1})$ and the displacement under the force is rotated by R.

$$\overline{C}' = \left(\begin{array}{c|c} R & 0 \\ \hline 0 & R \end{array}\right) \overline{C} \left(\begin{array}{c|c} R^T & 0 \\ \hline 0 & R^T \end{array}\right) \tag{11}$$

For both coordinate transformations, the compliance matrix is multiplied by transformation matrix and its transposed matrix from the left and right sides. The following operation is defined.

$$\overline{A} \otimes \overline{C} = \overline{A}\,\overline{C}\,\overline{A}^T \tag{12}$$

The following matrix functions are also defined. The $R_x(\theta)$, $R_y(\theta)$, and $R_z(\theta)$ means the θ rotation around

x-, y-, and z-axes, respectively. P and I are same as mentioned previously.

$$\overline{R}_{x,y,z}(\theta) = \left(\begin{array}{c|c} R_{x,y,z}(\theta) & 0 \\ \hline 0 & R_{x,y,z}(\theta) \end{array}\right) \quad (13)$$

$$\overline{P}(p_x, p_y, p_z) = \left(\begin{array}{c|c} I & P^T \\ \hline 0 & I \end{array}\right) \quad (14)$$

3 Kinematic Analysis of Translational 3-DOF Micro Parallel Mechanism

3.1 Translational 3-DOF Micro Parallel Mechanism

This subsection briefly introduces our translational 3-DOF micro parallel mechanism. As shown in Fig. 4, the end-plate is supported by 3 chains of links, and each chain has 3 parallelepiped mechanisms (See Fig. 5). These parallelepiped mechanisms keep the end-plate in parallel to the base. All angular joints of parallelepiped mechanism are right circular notched hinges. The piezo actuator pushes the middle plate of the chain indicated by an arrow in Fig. 4 and generates a micro-motion of the end-plate.

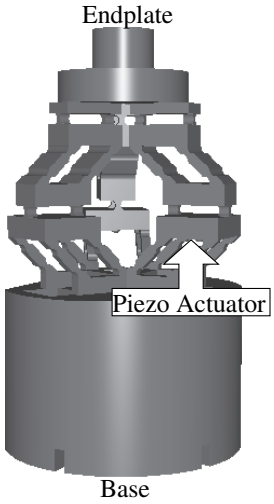

Figure 4: Translational 3-DOF Micro-Parallel Mechanism

If all hinges were ideal angular joints and other mechanical members are ideally rigid, the motion would be ideally translational. In fact, rotational motions are generated by stiffness of hinges and elasticity of links. This fact motivates us to analyze the error effect of hinges and links to the end-plate.

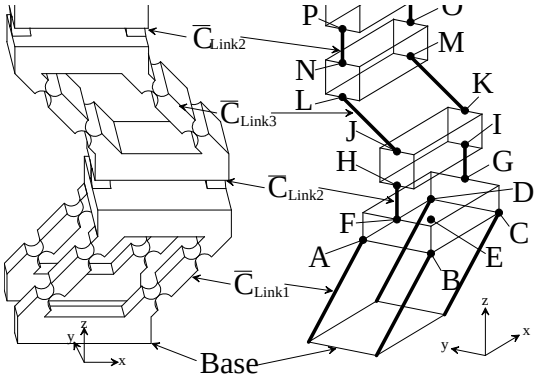

Figure 5: 1 Chain of Micro-Parallel Mechanism

Here, the smaller matrix is built step by step. This method can be easily understood.

3.2 Compliance Matrix of Translational 3-DOF Micro Parallel Mechanism

This mechanism consists of 3 chains. The structure of a chain and notations of its nodes are shown in Fig. 5. It is assumed that the members of ABCDEFG, HIJK, LMNO, and PQR are rigid enough to be treated as rigid body. Unless ABCDEFG is rigid body, this structure cannot be treated as frame structure. This is approximation to Rahmen structure. In case that ABCDEFG is elasticity member, the analysis is possible but difficult.

Hereafter, $\overline{C}_{ABCD}$ means the compliance matrix of ABCD. $\overline{C}_{prism}(a,b,l)$ and $\overline{C}_{hinge}(r,t,b)$ are compliance matrices of prismatic beam shown in Fig. 2(b) and circular notched hinge shown in Fig. 2(c), respectively. F_A and X_A are the forces on A and displacement of A, $\overline{P}_{EF}$ is coordinate transformation matrix from E to F.

The compliance matrices of $\overline{C}_{Link1}$ and $\overline{C}_{Link2}$, which are shown in Fig. 6, are obtained in Eq. (15) and Eq. (16). $\overline{C}_{Link3}$ is omitted here because it's nearly similar to $\overline{C}_{Link1}$.

$$\begin{aligned} \overline{C}_{Link1} = & \overline{P}(0,0,n_1+2r_1+l_1+2r_1) \otimes \overline{C}_{prism}(a_1,b_1,n_1) \\ + & \overline{P}(0,0,n_1+2r_1+l_1) \otimes \overline{C}_{hinge}(r_1,t_1,b_1) \\ + & \overline{P}(0,0,n_1+2r_1) \otimes \overline{C}_{prism}(a_1,b_1,l_1) \\ + & \overline{P}(0,0,n_1) \otimes \overline{C}_{hinge}(r_1,t_1,b_1) \\ + & \overline{C}_{prism}(a_1,b_1,n_1) \end{aligned} \quad (15)$$

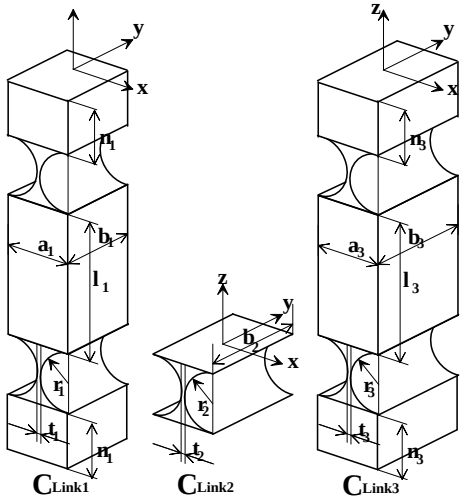

Figure 6: Elements of chain

$$\overline{C}_{Link2} = \overline{C}_{hinge}(r_2, t_2, b_2) \quad (16)$$

$\overline{C}_{ABCD}$ is statically determinate because the structure ABCD has no closed loop.

$$\overline{C}_{ABCD} = \begin{pmatrix} \overline{C'}_{Link1} & 0 & 0 & 0 \\ 0 & \overline{C'}_{Link1} & 0 & 0 \\ 0 & 0 & \overline{C'}_{Link1} & 0 \\ 0 & 0 & 0 & \overline{C'}_{Link1} \end{pmatrix} \quad (17)$$

Nothing that $\overline{C'}_{Link1} = \overline{R}_y(\pi/4) \otimes \overline{C}_{Link1}$

Because ABCDEFG is rigid body, relative displacements don't occur among A, B, C, D, E, F, G. The equilibriums of displacements lead Eq. (18) and (19).

$$\begin{pmatrix} \overline{P}_{EA} \\ \overline{P}_{EB} \\ \overline{P}_{EC} \\ \overline{P}_{ED} \end{pmatrix} X_E = \begin{pmatrix} X_A \\ X_B \\ X_C \\ X_D \end{pmatrix} = \overline{C}_{ABCD} \begin{pmatrix} F_A \\ F_B \\ F_C \\ F_D \end{pmatrix} \quad (18)$$

$$\begin{pmatrix} X_E \\ X_F \\ X_G \end{pmatrix} = \begin{pmatrix} \overline{I} \\ \overline{P}_{EF} \\ \overline{P}_{EG} \end{pmatrix} X_E \quad (19)$$

The equilibriums of forces lead Eq. (20).

$$\begin{pmatrix} \overline{P}_{EA}^T & \overline{P}_{EB}^T & \overline{P}_{EC}^T & \overline{P}_{ED}^T \end{pmatrix} \begin{pmatrix} F_A \\ F_B \\ F_C \\ F_D \end{pmatrix} = \begin{pmatrix} \overline{I} & \overline{P}_{EF}^T & \overline{P}_{EG}^T \end{pmatrix} \begin{pmatrix} F_E \\ F_F \\ F_G \end{pmatrix} \quad (20)$$

Then the new compliance matrix of EFG can be obtained.

$$\overline{C}_{EFG} = \begin{pmatrix} \overline{I} \\ \overline{P}_{EF} \\ \overline{P}_{EG} \end{pmatrix} \otimes \left(\begin{pmatrix} \overline{P}_{EA}^T & \overline{P}_{EB}^T & \overline{P}_{EC}^T & \overline{P}_{ED}^T \end{pmatrix} \otimes (\overline{C}_{ABCD})^{-1} \right)^{-1} \quad (21)$$

Then the compliance matrix of one chain, $\overline{C}_{ER}$, can be obtained through Eq. (22)-(27). In the same manner, the compliance matrix of parallel mechanism can be obtained through Eq. (28)-(31). These calculations are routine jobs.

$$\overline{C}_{EHI} = \begin{pmatrix} \overline{I} & 0 & 0 \\ 0 & \overline{P}_{FH} & 0 \\ 0 & 0 & \overline{P}_{GI} \end{pmatrix} \otimes \overline{C}_{EFG} + \begin{pmatrix} 0 & 0 & 0 \\ 0 & \overline{C'}_{Link2} & 0 \\ 0 & 0 & \overline{C'}_{Link2} \end{pmatrix} \quad (22)$$

$$\overline{C}_{EJK} = \begin{pmatrix} \overline{I} & 0 \\ 0 & \overline{I} \\ 0 & \overline{P}_{JK} \end{pmatrix} \otimes \left(\begin{pmatrix} I & 0 & 0 \\ 0 & \overline{P}_{JH}^T & \overline{P}_{JI}^T \end{pmatrix} \otimes (\overline{C}_{EHI})^{-1} \right)^{-1} \quad (23)$$

$$\overline{C}_{ELM} = \begin{pmatrix} \overline{I} & 0 & 0 \\ 0 & \overline{P}_{JL} & 0 \\ 0 & 0 & \overline{P}_{KM} \end{pmatrix} \otimes \overline{C}_{EJK} + \begin{pmatrix} 0 & 0 & 0 \\ 0 & \overline{C'}_{Link3} & 0 \\ 0 & 0 & \overline{C'}_{Link3} \end{pmatrix} \quad (24)$$

$$\overline{C}_{ENO} = \begin{pmatrix} \overline{I} & 0 \\ 0 & \overline{I} \\ 0 & \overline{P}_{NO} \end{pmatrix} \otimes \left(\begin{pmatrix} I & 0 & 0 \\ 0 & \overline{P}_{NL}^T & \overline{P}_{NM}^T \end{pmatrix} \otimes (\overline{C}_{ELM})^{-1} \right)^{-1} \quad (25)$$

$$\overline{C}_{EPQ} = \begin{pmatrix} \overline{I} & 0 & 0 \\ 0 & \overline{P}_{NP} & 0 \\ 0 & 0 & \overline{P}_{OQ} \end{pmatrix} \otimes \overline{C}_{ENO} + \begin{pmatrix} 0 & 0 & 0 \\ 0 & \overline{C'}_{Link2} & 0 \\ 0 & 0 & \overline{C'}_{Link2} \end{pmatrix} \quad (26)$$

$$\overline{C}_{ER} = \left(\begin{pmatrix} I & 0 & 0 \\ 0 & \overline{P}_{RP}^T & \overline{P}_{RQ}^T \end{pmatrix} \otimes (\overline{C}_{EPQ})^{-1} \right)^{-1} \quad (27)$$

Noting that $\overline{C'}_{Link3} = \overline{R}_y(-\pi/4) \otimes \overline{C}_{Link3}$
$\overline{C'}_{Link2} = \overline{R}_z(\pi/2) \otimes \overline{C}_{Link2}$

$$\overline{C}_{E1R1} = \overline{C}_{ER} \quad (28)$$

$$\overline{C}_{E2R2} = \begin{pmatrix} \overline{R}_z(2\pi/3) & 0 \\ 0 & \overline{R}_z(2\pi/3) \end{pmatrix} \otimes \overline{C}_{ER} \quad (29)$$

$$\overline{C}_{E3R3} = \begin{pmatrix} \overline{R}_z(-2\pi/3) & 0 \\ 0 & \overline{R}_z(-2\pi/3) \end{pmatrix} \otimes \overline{C}_{ER} \quad (30)$$

$$\overline{C}_{E1E2E3R} = \left(\begin{pmatrix} I & 0 & 0 & 0 & 0 & 0 \\ 0 & 0 & I & 0 & 0 & 0 \\ 0 & 0 & 0 & 0 & I & 0 \\ 0 & I & 0 & I & 0 & I \end{pmatrix} \otimes \begin{pmatrix} \overline{C}_{E1R1} & 0 & 0 \\ 0 & \overline{C}_{E2R2} & 0 \\ 0 & 0 & \overline{C}_{E3R3} \end{pmatrix}^{-1} \right)^{-1} \quad (31)$$

4 Analysis Results and Discussions

The minimum thickness t of circular notched hinge, (See Fig. 2(c)), is the dominant factor of its flexibility. If t was infinitesimal, the hinges worked as ideal angular joint and the end-plate moves translationally. As reported in [8], however, the rotational displacements of end-plate are generated by the counter moment of the hinge.

Fig. 7 explains that M_{hinge}, which is necessary to bend the hinge, causes the counter force F_{link} on the other link and that the end-plate is lifted by F_{link}. The rotational motion can be observed by the displacement of the tip of needle, whose length is l_{needle}. This needle is the end-effector of this manipulator. If rotational motion θ_y occurs, the tip of needle moves $\theta_y\, l_{needle} + \delta_x$. Actually, this error is profitable because it extends the workspace.

Eq. (32) shows the theoretical forward kinematics, the relationship between the inputs and translational displacements of the tip of needle. l_{E1}, l_{E2}, and l_{E3}

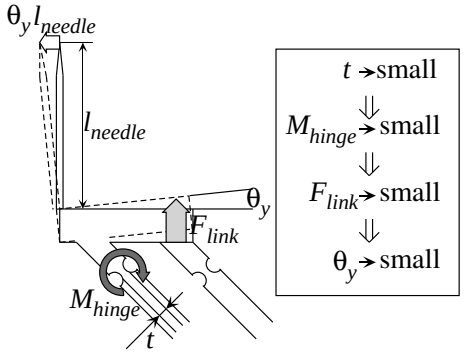

Figure 7: Rotational Displacements of Endplate

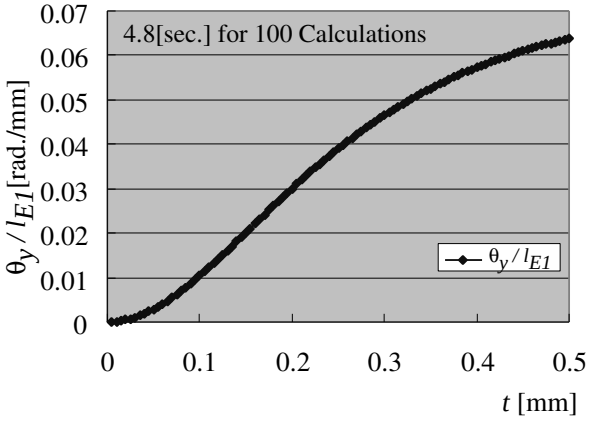

Figure 8: Elements of chain

are the elongations of piezo actuators, namely the displacements of middle plate in z-axis. The dimensions of this micro parallel mechanism are omitted here, but simply $l_1 = l_3 = 2.0$[mm], $b_1 = 1.1$[mm], $b_3 = 3.6$[mm], $r_1 = r_2 = r_3 = 0.5$[mm], $l_{needle} = 80.0$[mm]. Theoretically, the rotational displacement doesn't occur, so the displacement of needle is same as that of end-plate.

$$\begin{pmatrix} \delta_x \\ \delta_y \\ \delta_z \end{pmatrix} = \begin{pmatrix} -1.33 & 0.67 & 0.67 \\ 0 & -1.15 & 1.15 \\ 0.67 & 0.67 & 0.67 \end{pmatrix} \begin{pmatrix} l_{E1} \\ l_{E2} \\ l_{E3} \end{pmatrix} \quad (32)$$

Eq. (33) shows the forward kinematics calculated by our matrix method while t is infinitesimal, namely $t = 0.005$. The calculation is verified to be correct because the matrix is almost similar to Eq. (32).

$$\begin{pmatrix} \delta_x \\ \delta_y \\ \delta_z \end{pmatrix} = \begin{pmatrix} -1.32 & 0.66 & 0.66 \\ 0.0 & -1.14 & 1.14 \\ 0.68 & 0.68 & 0.68 \end{pmatrix} \begin{pmatrix} l_{E1} \\ l_{E2} \\ l_{E3} \end{pmatrix} \quad (33)$$

Fig. 8 shows the ratio of rotational displacement θ_y to input length l_{E1} while t is increased from 0.005[mm] to 0.5[mm]. As t increased, the error motion of the end-plate is increased. 100 calculations of our matrix method are performed in 4.8[sec.] (48[msec.] for 1 calculation) with Intel Pentium II 450MHz Xeon. This fact proves that our matrix method is so fast that it can be applicable to qualitative analysis of flexure mechanism. (Suppose that in case of FEM, modeling, meshing, and calculation take much longer time.)

Eq. (34) shows the actual forward kinematics measured in the calibration experiment. And Eq. (35) shows the forward kinematics calculated by our matrix methods while t is set to the designed value, 0.5[mm].

The difference between designed and actual parameters, and approximation to Rahmen structure might affect on the calculation. In this simulation, only f_z effects on the middle plate of the chain and the motion in other axes is allowed. However, the friction between the middle plate and piezo actuator prevents these motions. These might cause error of simulation.

$$\begin{pmatrix} \delta_x \\ \delta_y \\ \delta_z \end{pmatrix} = \begin{pmatrix} -4.39 & 2.27 & 2.13 \\ -0.10 & -3.38 & 3.41 \\ 0.74 & 0.70 & 0.57 \end{pmatrix} \begin{pmatrix} l_{E1} \\ l_{E2} \\ l_{E3} \end{pmatrix} \quad (34)$$

$$\begin{pmatrix} \delta_x \\ \delta_y \\ \delta_z \end{pmatrix} = \begin{pmatrix} -6.82 & 3.41 & 3.41 \\ 0.0 & -5.90 & 5.90 \\ 0.44 & 0.44 & 0.44 \end{pmatrix} \begin{pmatrix} l_{E1} \\ l_{E2} \\ l_{E3} \end{pmatrix} \quad (35)$$

5 Summary and Conclusions

We applied the matrix method to the analysis of our translational 3-DOF micro parallel mechanism for an instance of general flexure mechanisms. While this analysis, we assumed that

1. Linearization between force and deformation (Hook's law)
2. Linearization of translational and rotational displacements
3. Approximation to Rahmen structure

Firstly, the compliance matrices of a right circular notched hinge and other members are defined. Secondly the coordinate transformations are described. Thirdly, the compliance matrix of translational 3-DOF micro parallel mechanism is obtained. Fourthly, the affection of rigidity of the right circular notched hinge to the rotational displacement is analyzed and it was proved that this method is very rapid.

We expect this method is applicable to some other micro flexure mechanism.

References

[1] J. M. Paros and L. Weisbord, "How to design Flexure Hinges", Machine Design, 37, pp. 151-156, November 25, 1965

[2] Y. Yoshimura, "Analysis on Stiffness of Elastic Hinges" J. of Japan Society for Precision Engineering, Vol. 64, No. 11, pp. 1589-1593, 1998 (in Japanese)

[3] Y. Rong, Y. Zhu, Z. Luo, X. Liu, "Design and Analysis of Flexure-Hinge Mechanism Used in Micro-Positioning Stages", ASME, PED-Vol.68-2, Manufacturing Science and Engineering, pp. 979-986, 1994

[4] I. Her and J. C. Chang, "A Linear Scheme for the Displacement Analysis of Micropositioning Stages with Flexure Hinges", Trans. of the ASME, Journal of Mechanical Design, Vol. 116, pp. 770-776, 1994

[5] A. Hara and K. Sugimoto, "Synthesis of Parallel Micromanipulators", Trans. of the ASME, Journal of Mechanisms, Transmissions and, Automation in Design, Vol. 111, pp. 34-39, 1989

[6] E. C. Pestel, F. A. Leckie, "Matrix Methods in Elasto Mechanics", McGraw-Hill Book Co., Inc., New York, 1963

[7] H. C. Martin, "Introduction to Matrix Methods of Structural Analysis", McGraw-Hill Book Co., Inc., New York, 1966

[8] T. Tanikawa, T. Arai, N. Koyachi, "Development of Small-sized 3 DOF Finger Module in Micro Hand for Micro Manipulation", Proc. IEEE/RSJ IROS, pp. 876-881, Oct. 17-21, 1999